IRON BASED SUPERCONDUCTORS

By
NAHOM TEFERA

A PROJECT SUBMITTED TO THE SCHOOL OF GRADUATE STUDIES ADDIS ABABA UNIVERSITY

SUBMITTED IN PARTIAL FULFILLMENT OF THE
REQUIREMENTS FOR THE DEGREE OF
MASTER OF SCIENCE
AT
ADDIS ABABA UNIVERSITY
ADDIS ABABA,ETHIOPIA
JUNE 2012

© Copyright by Nahom Tefera, JUNE 2012

ADDIS ABABA UNIVERSITY
DEPARTMENT OF
PHYSICS

The undersigned hereby certify that they have read and recommend to the School of Graduate Studies for acceptance a project entitled "**IRON BASED SUPERCONDUCTORS**" by **Nahom Tefera** in partial fulfillment of the requirements for the degree of **Master of Science**.

Dated: June 2012

Supervisors:

Prof. Singh P.

First Readers:

Prof. Malnev V.

ADDIS ABABA UNIVERSITY

Date: **June 2012**

Author: **Nahom Tefera**

Title: **IRON BASED SUPERCONDUCTORS**

Department: **Physics**

Degree: **M.Sc.** Convocation: **June** Year: **2012**

Permission is herewith granted to Addis Ababa University to circulate and to have copied for non-commercial purposes, at its discretion, the above title upon the request of individuals or institutions.

Signature of Author

THE AUTHOR RESERVES OTHER PUBLICATION RIGHTS, AND NEITHER THE THESIS NOR EXTENSIVE EXTRACTS FROM IT MAY BE PRINTED OR OTHERWISE REPRODUCED WITHOUT THE AUTHOR'S WRITTEN PERMISSION.

THE AUTHOR ATTESTS THAT PERMISSION HAS BEEN OBTAINED FOR THE USE OF ANY COPYRIGHTED MATERIAL APPEARING IN THIS THESIS (OTHER THAN BRIEF EXCERPTS REQUIRING ONLY PROPER ACKNOWLEDGEMENT IN SCHOLARLY WRITING) AND THAT ALL SUCH USE IS CLEARLY ACKNOWLEDGED.

Contents

List of Figures

List of Tables

Acknowledgements

Above all, I would like to thank the almighty God, Then I would like to express my sincere thanks to my advisor and instructor Prof. Singh for his guidance, assistance, supervision and contribution of valuable suggestions.

Abstract

This project is well organized review of new class of high-T_c superconductors i.e iron-based layered compounds such as $ReOFeAs$ (Re is a rare-earth element), AFe_2As_2 (A = Ba, Sr, Ca), and $LiFeAs$, all of which are becoming superconducting with the current maximum T_c up to 55 K. The crystal and electronic structure, and magnatic properties all these compounds were discussed. In this paper, the superconducting properties of such systems are reviewed in detail, including the dependence of T_c on the doping level, and external pressure.

In this project we discussed about the pairing symmetry and possible mechanism of superconductivity of iron based superconductors. we also discussed the progress and potential application of iron based superconductors.

Chapter 1

Introduction

A perfect superconductor is a material that exhibits two characteristic properties, namely zero electrical resistance and perfect diamagnetism, when it is cooled below a particular temperature T_c called the critical temperature. At higher temperatures it is a normal metal, and ordinarily is not a very good conductor. For example, lead, tantalum, and tin become superconductors, while copper, silver, and gold, which are much better conductors, do not super-conduct.

Perfect diamagnetism, the second characteristic property, means that a superconducting material does not permit an externally applied magnetic field to penetrate into its interior. Those superconductors that totally exclude an applied magnetic flux are known as Type I superconductors, and Other superconductors, called Type II superconductors, are also perfect conductors of electricity, but their magnetic properties are more complex. They totally exclude magnetic flux when the applied magnetic field is low, but only partially exclude it when the applied field is higher.

1.1 Brief History of Superconductivity

The history of superconductivity have date back 100 years, It begins in 1908, where H. Kamerlingh Onnes initiated the field of low-temperature physics by liquefying helium in his laboratory at Leiden. Three years later he found that below 4.15 K of the DC resistance of mercury dropped to zero [1]. With that finding the field of superconductivity was born. Two year later, in 1913, the element lead was found to be superconducting at 7.2 K. After 17 years were to pass the element niobium was found to be superconducting at $T_c = 9.2$ K.

A considerable amount of time went by before physicists became aware of the second distinguishing characteristic of a superconductor namely, its perfect diamagnetism. In 1933, Meissner and Ochsenfeld found that when a sphere is cooled below its transition temperature in a magnetic field, it excludes the magnetic flux [2]. The report led the London brothers, Fritz and Heinz, to propose equations that explain this effect and predict how far a static external magnetic field can penetrate into a superconductor [3]. The next theoretical advance came in 1950 with the theory of Ginzburg and Landau, which described superconductivity in terms of an order parameter and provided a derivation for the London equations [4].

In the same year it was predicted theoretically by H. Fröhlich that the T_c would decrease as the average isotopic mass increased [5]. this effect,called the **Isotope effect**,was observed experimentally the same year by Maxwell [6]. The isotope effect provided support for the electron-phonon interaction mechanism of superconductivity [7].

Our present theoretical understanding of the nature of superconductivity is based on the BCS microscopic theory proposed by J. Bardeen, L. Cooper, and R. Schrieffer in 1957 [8]. In this theory it is assumed that bound electron pairs that carry the super-current are formed

and that an energy gap between the normal and super-conductive states is created. The Ginzburg–Landau and London's results fit well into the BCS formalism. The present theoretical debate centers around how well the BCS theory explains the properties of high temperature superconductors.

On April 17, 1986, an article, entitled "Possible High T_c Superconductivity in the Ba-La-Cu-O System," written by J. G. Bednorz and K. A. Müller was received by the "Zeitschrift für Physik" which is Journal of Physical Chemistry, initiating the era of high-temperature superconductivity [9].Sharp drops in resistance attributed to "high-Tc " superconductivity had appeared from time to time over the years, but when examined they had always failed to show the required diamagnetic response or were otherwise unsubstantiated.

By the beginning of 1987, scientists had discover the lanthanum compound, which went superconducting at close to 40 K at atmospheric pressure and at up to 52 K under high pressure [10]. Soon thereafter, the yttrium-barium system, which went superconducting in the 90K was discovered [11]. Early in 1988, superconductivity reached 110 K with the discovery of BiSr-CaCuO [12] and then the 120-125 K range with TiBa-CaCuO [13]. More recently in 1993 scientists reported T_c of 131.8 K for $Tl_2Ba_2Ca_2Cu_3O_{10-x}$ at a pressure of 7GPa and the highest-temperature superconductor (at ambient-pressure) is mercury barium calcium copper oxide ($HgBa_2Ca_2Cu_3O_x$), at which possibly 135 K and is held by a cuprate-perovskite material, reaches 164 K under high pressure [14, 15].

This rapid change and improvement in superconductors exceeds that of earlier decades, For 56 years the element niobium and its compounds had dominated the field of superconductivity by providing the highest T_c values. The period from 1930 to 1986 can be called the Niobium Era

of superconductivity. The period that began in 1986 become the Copper Oxide Era because, thus far, the presence of copper and oxygen has, with rare exceptions, been found essential for high T_c and Iron-based superconductors is currently the family with the second highest critical temperature, behind the cuprates. Interest in their superconducting properties began in 2006 with the discovery of superconductivity in LaOFeP at 3.5 K [16]and gained much greater attention in 2008 after the analogous material LaFeAs(O,F) was found to super-conduct at up to 43 K under pressure [17, 18]. Later, by substituting other rare-earth elements for Lanthanum, several Chinese researchers obtained considerably higher values ($T_c = 41 KinCeO_{1-x}F_xFeAs$ [19], $T_c = 52 KinPrO_{1-x}F_xFeAs$ [20]) and reached $T_c = 55$ K in $SmO_{1-x}F_xFeAs$ [21]. Different Alloys and compounds have been discovered and extensively studied, shown in figure 1.1.

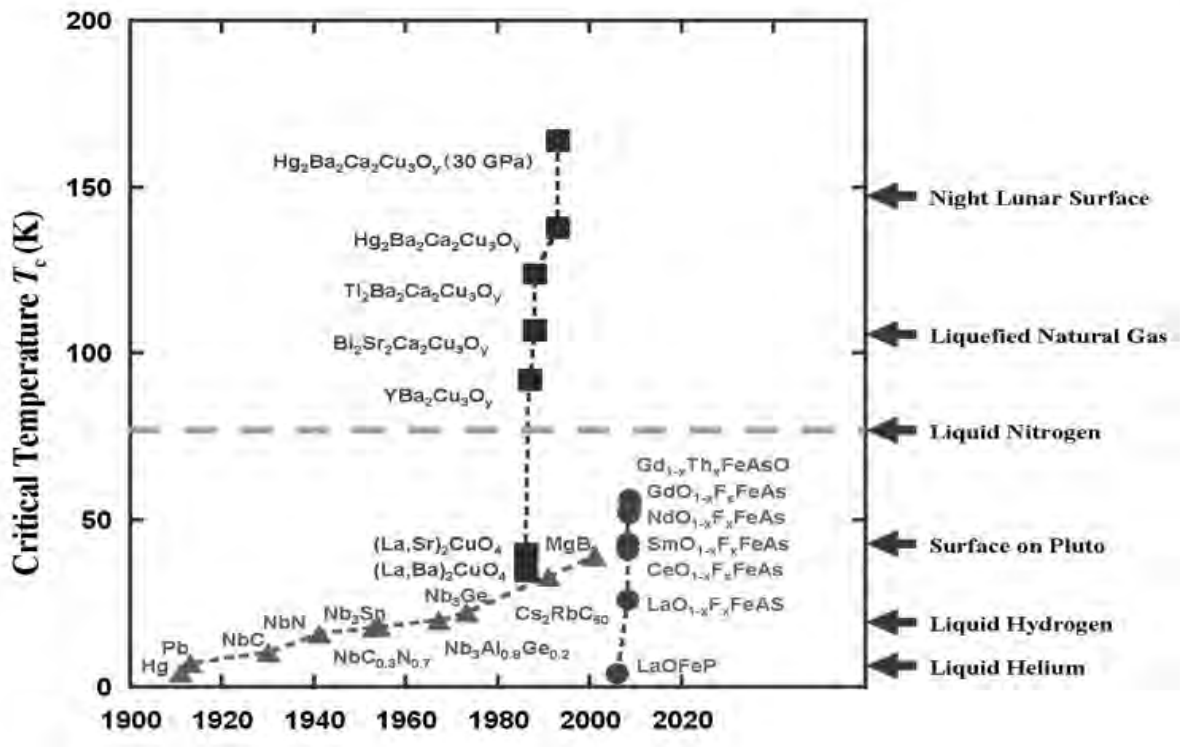

Figure 1.1: The year of superconductors discovery and their T_c.

Chapter 2

Literature Review

2.1 Superconductivity

2.1.1 ZERO Electrical Resistance

At 4.3 K the mercury was superconducting; Onnes expected that if he turned off the voltage, the current stopped flowing, but, He noticed that even if he turned off the voltage below 4.2 K, the current continued to flow! In fact the current continues to flow without loss for months and years. The resistance of the material had become zero. The state of matter in which resistance is zero is known as the superconducting state. this zero resistance is the first characteristic property of a superconductors. The figure shows a plot of Onnes's original resistance measurements, the first observation of superconductivity. We see that resistance drops sharply over a very narrow temperature range, from 0.11 ohm at 4.22 K to 0.00001 ohm ($10^{-5} ohm$) at 4.19 K.

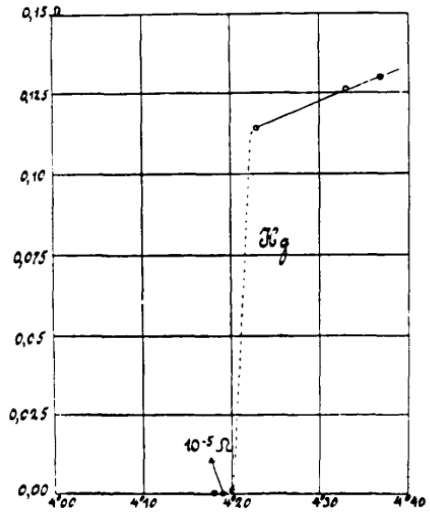

Figure 2.1: H.K Onnes's original resistance Vs temperature plot.

2.1.2 Meissner effect

The second characteristic of the superconducting state, in addition to that of zero resistance, is called the Meissner effect [2]. It is the expulsion of a magnetic field from a superconductor during its transition to the superconducting state. superconductors in the Meissner state exhibit perfect diamagnetism, meaning that the total magnetic field is very close to zero deep inside the superconductor. According to Lenz's law a current generated, which oppose the flux, and Canceled out any magnetic field from the superconductors.

We can show how superconductor exhibit perfect diamagnetic property

$$B = \mu_o(H + M) \tag{2.1}$$

Where M is magnetization, H is magnetic field and μ_o is the permeability of free space.

$$\chi = \frac{M}{H} \tag{2.2}$$

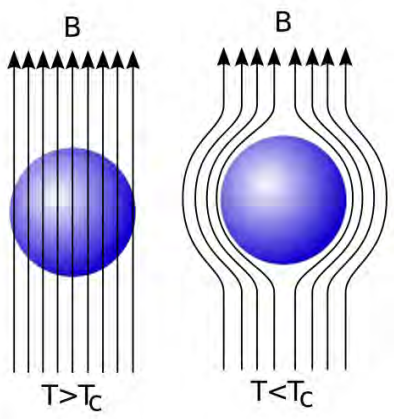

Figure 2.2: Diagram of the Meissner effect.

where χ is magnetic susceptibility then

$$B = \mu_o H(1 + \chi) \tag{2.3}$$

In case superconductors B = 0, so that $\chi = -1$. These show that superconductors are perfect diamagnet.

2.1.3 London equation

The London equations relate current to electromagnetic fields in and around superconductor [3]. It is the simplest description of superconducting phenomena. It correctly predict magnetic field penetration into the superconducting material and ability to explain the Meissner effect.

Let assume a two fluid model where we distinguish between normal and superconducting electrons.

$$n = n_n + n_s \tag{2.4}$$

Where n is density of electron, n_n and n_s is density of normal state and superconducting state,

respectively. For superconducting electrons in electronic field we can write

$$m^* \frac{\partial V_s}{\partial t} = -e^* E \tag{2.5}$$

If we consider equation for current density and apply it for superconducting electron.

$$j_s = -n_s e^* V_s \tag{2.6}$$

We get

$$\frac{\partial j_s}{\partial t} = \frac{n_s e^{*2}}{m^*} E \tag{2.7}$$

combining this with Maxwell equation

$$\nabla \times E = -\frac{\partial B}{\partial t} \tag{2.8}$$

we get

$$\frac{\partial}{\partial t}\left(\frac{n_s e^{*2}}{m^*} B + \nabla \times j_s\right) = 0 \tag{2.9}$$

Assuming the expression in the parentheses is zero, we obtain the following equation

$$\frac{n_s e^{*2}}{m^*} B + \nabla \times j_s = 0 \tag{2.10}$$

Equations 2.7 and 2.10 are called the first and second London equations, respectively. Again, combined with

$$\nabla \times j_s = -\frac{c}{4\pi} \nabla^2 B \tag{2.11}$$

we have

$$\nabla^2 B - \frac{1}{\lambda_L^2} B = 0 \tag{2.12}$$

$$B(x) = B_o e^{-x/\lambda_L} \tag{2.13}$$

Where $\lambda_L = (\frac{m^*}{\mu_o n_s e^{*2}})^{1/2}$ is a London penetration depth, which measures the of penetration of the magnetic field.

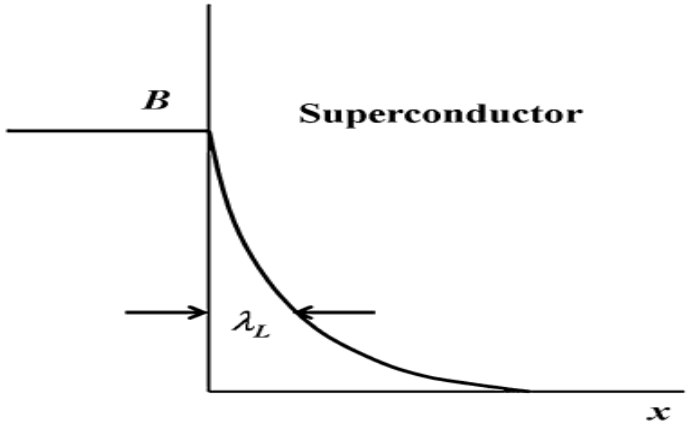

Figure 2.3: London penetration depth inside superconductor.

2.1.4 Type of Superconductors

Superconductors are differentiated by there magnetization curves i.e. TYPE I and TYPE II Superconductor.

Type-I superconductors :- In Type I, as the external magnetic flux density H_{app} is increased, it does not penetrate the bulk of the material in the superconducting state until a field is reached the critical field H_c, above which the superconducting state no longer exists. superconductivity is abruptly destroyed during a first order phase transition when the strength of the applied field rises above a critical value H_c. As such, they have only a single critical

magnetic field at which the material stop to super-conduct, becoming resistive. Elementary superconductors, such as aluminum and lead are typical Type-I superconductors. The origin of their superconductivity is explained by BCS theory. This type of superconductivity is normally exhibited by pure metals, e.g aluminum, lead or mercury.

Type-II superconductors :- In a Type II superconductor there is no magnetic field H_{in} inside the material until a field H_{c1} is reached, referred to as the lower critical field. At H_{c1} flux density begins to penetrate the sample but does not remove all of the superconducting state. As the field is further increased to a value H_{c2} referred to as the upper critical field, more flux density continues to penetrate the sample. At H_{c2} the superconducting state is totally removed. Generally these superconductor characterized by the formation of vortex lattices in magnetic field and they have a continuous second order phase transition from the superconducting to the normal state within an increasing magnetic field. Type-II superconductors are usually made of metal alloys or complex oxide ceramics,While most pure metal superconductors are Type-I,exceptionally niobium, vanadium and technetium are pure element Type-II superconductors.

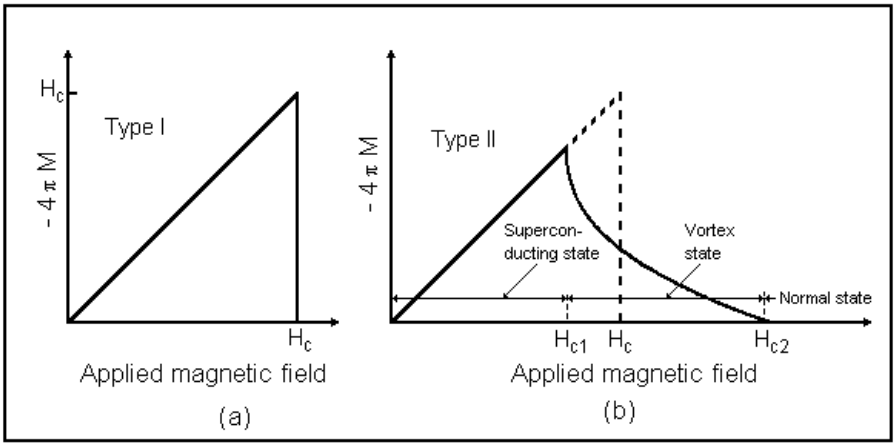

Figure 2.4: Magnetization curves of Type I and Type II superconductors.

We can also differentiate Type of superconductors using the Ginzburg–Landau parameter.

$$K = \frac{\lambda}{\xi} \tag{2.14}$$

Where ξ is coherence length and λ is penetration depth

It has been shown that Type I superconductors are those with $K < 1/\sqrt{2}$, and Type II superconductors those with $K > 1/\sqrt{2}$.

2.1.5 Quantization of magnetic field

The magnetic flux quantum Φ_o is the quantum of magnetic flux passing through a superconductor. the flux passing through any area bounded by such current is quantized. The quantum of magnetic flux is a physical constant, as it is independent of the underlying material as long as it is a superconductor. Its value is $\Phi_o = \mathrm{h}/(2\mathrm{e}) = 2.067 \times 10^{-15}$ Weber. where h is Planck's constant and e is the elementary charge [22, 23]. The inverse of the flux quantum $1/\Phi_o$ is called the **Josephson constant**, and is denoted by K_J. It is the constant of proportionality of the Josephson effect, which is the phenomenon of supercurrent i.e. a current that flows indefinitely long without any voltage applied.

There are two main effects predicted by Josephson.

DC Josephson effect, it is phenomenon of a direct current crossing from the insulator in absence of any external electromagnetic field, owing to tunneling. This DC Josephson current is proportional to the sine of phase difference across the insulator.

AC Josephson effect, With a fixed voltage U_{DC} across junctions, the phase will vary linearly with time and the current will be an AC current with I_c and frequency $\frac{1}{h}2e \cdot U_{DC}$.

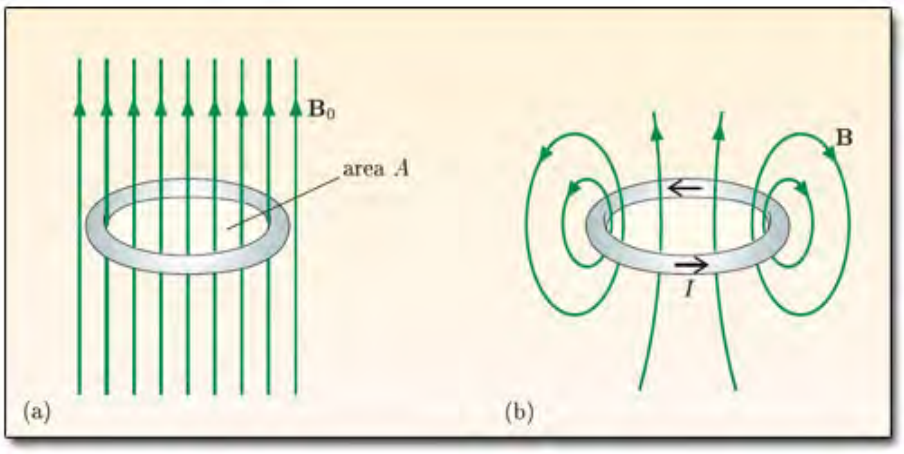

Figure 2.5: (a) A ring cooled below its critical temperature in an applied field B_o. (b) When the field is removed, a superconducting current maintains the flux through the ring at the same value.

To obtain the expression for Φ_o mentioned above, consider a small superconducting ring of radius R cooled to the superconducting state and carrying a super-current of density J. Since the wave function of every Cooper pair is in phase with that of every other pair, an exact integral multiple N of the wavelength λ of the pair is required to fit around the circumference $2\Pi R$ of the ring; otherwise the waves would not be coherent. the current in the ring is quantized with the quantization condition.

$$N\lambda = 2\pi R \tag{2.15}$$

Since λ = h/P where P is the momentum of a Cooper pair, we have in effect a Bohr like momentum quantization condition for the current in the ring.

$$Nh = 2\pi RP \tag{2.16}$$

The energy of a current flowing in a loop can be written in terms of the current I and the flux

Φ through the loop.

$$E = \frac{I\Phi}{2} \tag{2.17}$$

Since the current I for n electrons moving around the loop with velocity v is $\frac{nve}{2\pi R}$, where e is the electron charge, Eq. (2.16) becomes.

$$E = \frac{\Phi nev}{4\pi R} \tag{2.18}$$

The energy of n electrons moving around the ring can also be written.

$$E = \frac{nmv^2}{2} = \frac{nPv}{4} \tag{2.19}$$

where m is mass of the electron, P = 2mv is the momentum of a Cooper pair which contains two electrons. Comparing Eqs. (2.17) and (2.18) gives the momentum P.

$$P = \frac{\Phi e}{\pi R} \tag{2.20}$$

Substituting this into Eq. (2.15) and using the flux quantization condition $\Phi = N\Phi_o$ provides the expression for the unit quantum of flux.

$$\Phi_o = h/2e \tag{2.21}$$

which has the numerical value given at the beginning of this section.

2.1.6 Isotopic effect

Atoms of the same element with different weights are called isotopes; to explain a little about isotopes. The nucleus of an atom consists of two types of particles, namely, neutrons and protons. Protons are positively charged, and the number of protons in the nucleus equals the elements atomic number. The number of electrons orbiting the nucleus, which determines chemical and bonding characteristics, equals the number of protons. The neutron is neutral particles (no charge); the weight of an atom is proportional to the number of protons plus the number of neutrons. the main thing is how isotopes differ in their contribution to superconducting properties.

In 1950 H. Fröhlich concluded that vibrating atoms of a material must play an important role causing it to super-conduct. Fröhlich proposed that an electron-phonon interaction between electrons carrying the super-current and the lattice that vibrates bring about superconductivity. Where Lattice vibrations are a wavelike phenomenon associated with atoms of a solid oscillating in characteristic frequencies and these lattice vibrations is also called a **phonon**.

In this same year the experiment was carried out and found that the transition temperature decreased when the atom became heavier and the change was proportional to the reciprocal of the square root of the weight of the atom [6],

This may be expressed mathematically in generally form:

$$\frac{T_c}{T_c'} = \left(\frac{M'}{M}\right)^{\alpha} \tag{2.22}$$

Where the isotope effect exponent $\alpha = 0.5$and if $\alpha = 0$ if there is no isotope effect. Subsequent work showed that a number of other elemental superconductors also exhibit an isotope effect,

but some did so to a lesser extent than mercury, as indicated by data in Table 2.1.

Material	Symbol	T_c	α^a
Cadmium	Cd	0.5	0.5^a
Carbon(fullerene)		30	0.25
Lead	Pb	7.2	0.48
Mercury	Hg	4.1	0.5^a
Molybdenum	Mo	0.9	0.37
Osmium	Os	0.7	0.20
Rhenium	Re	1.7	0.23
Ruthenium	Ru	0.5	0^a
Thallium	TI	2.4	0.50^a
Tin	Sn	3.7	0.41
Zinc	Zn	0.9	0.45
Zirconium	Zr	0.6	0^a

[a] $\alpha = 0.5$ if the BCS phonon prediction is satisfied; $\alpha = 0$ if there is no isotope effect.

Table 2.1: Isotopic effect parameter for α for elementary superconductor.

These experimental results convinced physicists that a microscopic theory of superconductivity must involve the electron-phonon interaction to explain the isotope effect. Leon Cooper showed that two conduction electrons in the presence of very weak electron-phonon interaction are capable of forming the stable paired state referred to as a Cooper pair; this provided the final fact needed to formulate a microscopic theory of superconductivity.

2.1.7 High Temperature Superconductor

High-temperature superconductors are materials that have a superconducting transition temperature (T_c) above 30 K (-243.2 °C). From 1960 to 1980, 30 K was thought to be the highest theoretically possible T_c. As we discussed earlier the first high-T_c superconductor was discovered in 1986 by IBM researchers Karl Müller and Johannes Bednorz, for which they were awarded the Nobel Prize in Physics in 1987 [9]. The observation was reported for the compound La_2CuO_4 doped with small amounts of barium, with the formula $La_{2-x}Ba_xCuO_4$ which shows

superconductivity at 30 K.

Until Fe-based superconductors were discovered in 2008, the term high-temperature superconductor was used interchangeably with cuprate superconductor for compounds such as bismuth strontium calcium copper oxide (BSCCO) and yttrium barium copper oxide (YBCO).

The Yttrium-based Superconductor $YBa_2Cu_3O_{7-x}$ become Superconductor at 90 K, 13 degrees above the temperature at which liquid nitrogen boils.The superconducting properties of $YBa_2Cu_3O_{7-x}$ are sensitive to the value of x, its oxygen content. Only those materials with $0 \leq$ x ≤ 0.65 are superconducting below T_c, and when x$\sim$0.07 the material super-conducts at the highest temperature of 95 K, or in highest magnetic fields 120 T for B perpendicular and 250 T for B parallel to the CuO_2 planes. The replacement of copper in the planes by a transition ion such as Ni or by Zn reduces the transition temperature, and with high enough doping the superconductivity disappears. The deterioration of the superconductivity is greater with the addition of Zn than with Ni, hinting at the possible importance of the magnetic nature of the copper ion in the mechanism of superconductivity.

The Bismuth-based Superconductors one of family of copper oxide superconductors having the general formula $Bi_2Sr_2Ca_{n-1}Cu_nO_{2n+4}$,where n refers to the number of copper oxide planes per formula unit. Specific types of BSCCO are usually referred to using the sequence of the numbers of the metallic ions. Thus Bi-2201 is the n=1 compound ($Bi_2Sr_2CuO_{6+x}$), Bi-2212 is the n=2 compound ($Bi_2Sr_2CaCu_2O_{8+x}$) and Bi-2223 is the n=3 compound ($Bi_2Sr_2Ca_2Cu_3O_{10+x}$). when Growth of the n = 3 phase was facilitated by partial substitution of Pb for Bi, it giving a transition temperature of 113 K. In general there are a number of other variants of BSCCO superconducting families with critical temperature of Bi-2201 has $T_c \approx 20K$,Bi-2212

has $T_c \approx 95K$ and Bi-2223 has $T_c \approx 108K$. In the same year Thallium-based Superconductors also have been discovered with chemical formula $Tl_2Ba_2Ca_2Cu_3O_10$ (TBCCO-2223) has a critical temperature of 127 K, This series of compounds is isomorphic with the bismuth series, with Tl substituting for Bi, and Ba replacing Sr.

Among superconducting system the highest critical temperature belongs to Hg-Ba-Ca-Cu-O family, in this superconductors, the $HgBa_2Ca_2Cu_3O_{8+\delta}$ has highest critical temperature around 135 K at a normal pressure, and 164 K under pressure.

After more than twenty years of intensive research the origin of high-temperature superconductivity is still not clear, but it seems that instead of electron-phonon attraction mechanisms, as in conventional superconductivity, one is dealing with electronic mechanisms (e.g. by antiferromagnetic correlations), and instead of s-wave pairing, d-waves are substantial.

Transition temperature (in kelvins)	Material	Class
133	$HgBa_2Ca_2Cu_3O_x$	Copper-oxide superconductors
110	$Bi_2Sr_2Ca_2Cu_3O_{10}$ (BSCCO)	
90	$YBa_2Cu_3O_7$ (YBCO)	
77	Boiling point of liquid nitrogen	
55	SmFeAs(O,F)	Iron-based superconductors
41	CeFeAs(O,F)	
26	LaFeAs(O,F)	
20	Boiling point of liquid hydrogen	
18	Nb_3Sn	Metallic low-temperature superconductors
10	NbTi	
9.2	Nb	
4.2	Hg (mercury)	

Table 2.2: Transition temperatures of well-known superconductors.

2.1.8 Electron-Phonon Interaction

The attractive interaction between two electron is caused by the electron-phonon interaction supported by the discovery of isotopic effect on T_c showed that electron-phonon interaction plays an essential role in conventional superconductivity. This signifies that the lattice modes involved in superconductivity because of the dependency of T_c on the mass of the constituting atoms.

The electron-phonon interaction of the deformation potential type in a superconductors is given by the following Hamiltonian.

$$\hat{H} = \hat{H}_o + \hat{H}' \tag{2.23}$$

$$\hat{H}_o = \sum_{k\sigma} \epsilon_k a^\dagger_{k\sigma} a_{k\sigma} + \sum_q \hbar\omega_q b^\dagger_q b_q$$

$$\hat{H}' = i \sum_{kq\sigma} \chi_q a^\dagger_{k+q\sigma} a_{k\sigma} (b_q - b^\dagger_{-q})$$

Where

$\hat{H}_o$- Hamiltonian of electron and phonon with out mutual interaction.

$\hat{H}'$- coupling interaction.

$a^\dagger_{k\sigma} a_{k\sigma}$- are the creation (annihilation) operators of an electron specified by the wave vector K and spin σ and ϵ_k is the energy of one electron.

$b^\dagger_q b_q$- are creation (annihilation) operators of phonon labeled by the wave vector q, $\hbar\omega_q$ is the energy of phonon and χ_q is the coupling constant of electron-phonon interaction.

In the first order, $\hat{H}'$ causes electron-phonon scattering. in second order it leads to the above mentioned exchange of a phonon between electrons. This process illustrated in figure as

follow

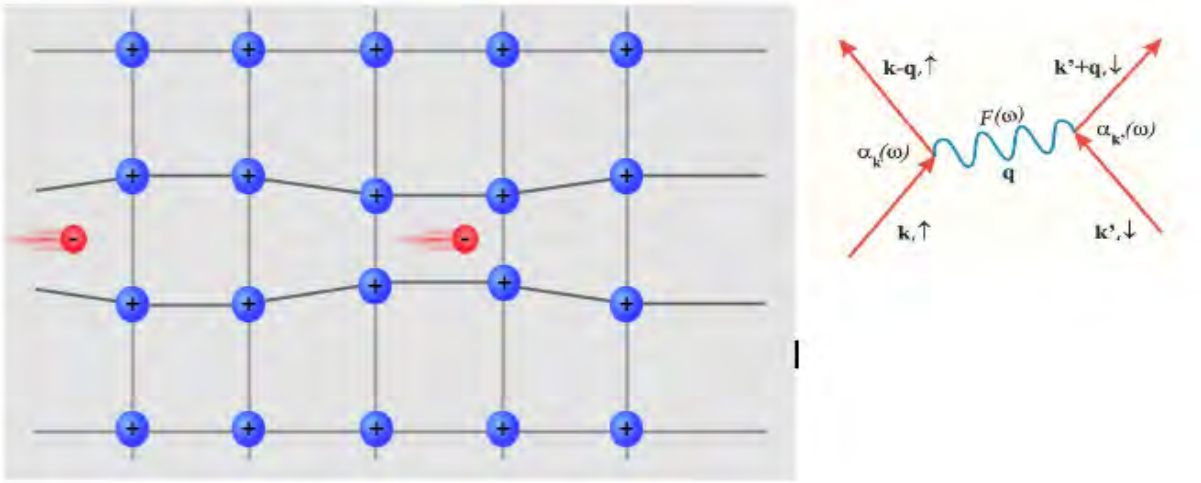

Figure 2.6: electron-phonon coupling

It shows that one electron polarizes the lattice and the other electron interacts with the polarized lattice. the expression of the attractive interaction can be found using canonical transformation which eliminates the first order term χ_q. so that the electron-phonon interaction written as

$$\hat{H}' = \sum_{kk'q\sigma\sigma'} |\chi_q|^2 a^\dagger_{k+q\sigma} a_{k\sigma} a^\dagger_{k'-q\sigma} a_{k'\sigma'} \frac{\hbar\omega_q}{(\epsilon_{k'} - \epsilon_{k'-q})^2 - (\hbar\omega_q)^2}$$

Such an attractive interaction is present in $\hat{H}'$ whenever $|\epsilon_{k'} - \epsilon_{k'-q}| < \hbar\omega_q$. this allow pairs of electrons to form a bound state of lower energy than that of the two free electrons. the existence of Cooper pairs in which two electron of opposite wave number and spin form a bound state, which provides the foundation for BCS Theory.

2.1.9 BCS Theory

In BCS theory of superconductivity they attributed superconductivity to an attractive interaction between two electrons through electron-phonon interaction. The attractive interaction between electrons can be understood in the following way: one electron interacts with a positive ion in the lattice and deforms the lattice; a second electron of compatible momentum value interacts with the ion in the distorted lattice so as to minimize the energy. The interacting electrons are said to form a pair.

The electrons of a pair have equal and opposite momentum (i.e. one with +k and other with –k), with the one in spin up state and the other in spin down state, so that the total spin of a pair is zero. The electron pairs are called **Cooper pairs**. The important feature of Cooper pair is that excitation can take place in only pairs of electrons; i.e., if the state with +k and spin up (↑) is occupied, the corresponding state with –k and spin down (↓) is also occupied and if the state of +k is vacant, the state of –k is also vacant. Two of the key experimental facts that led to the BCS understanding were:

- The density of states is gapped at the Fermi surface. This was determined experimentally first by the measurement of an exponential specific heat. This led to the realization that some kind of pairing is occurring (i.e. electrons are thermally activated across a gap with Boltzmann probability).

- Phonon's involvement was shown experimentally by the isotope effect; the critical temperature T_c was found to vary as the inverse square root of the nuclear mass, the discovery of the isotope effect led to the realization that phonon's are involved.

BCS theory also describe superconductivity as a microscopic effect caused by Bose-Einstein

condensation of pairs of electrons (Cooper pairs) in the presence of an attractive potential. The pairs with opposite spins act like bosons and leave an energy gap Δ between the BCS ground state and the first excited state.

$$\Delta = 2\hbar\omega_D e^{-1/V_o N_{E_f}} \tag{2.24}$$

where ω_D is Debye frequency, V_o is coupling potential and N_{E_f} is density of states of electron at the Fermi energy.

In its simplest form, BCS gives the superconducting transition temperature in terms of the electron-phonon coupling potential and the density of states of electron at the Fermi energy.

$$T_c K_B = 1.14\hbar\omega_D e^{-1/V_o N_{E_f}} \tag{2.25}$$

Chapter 3

Iron Based Superconductors

3.1 Ferropnictides

High-T_c superconductivity at 26 K was found by Kamihara group [17]. in Florine doped $LaFeAsO$ on February 2008. This was the discovery of high-T_c superconductivity in a entirely new class of materials that came to be known as iron-pnictides. This new type of superconductors is based on conducting layers of Iron and a Pnictide (typically Arsenic) and seems to show promise as the next stage of high temperature superconductors. Largely these materials have been called the **ferropnictides**.

Since after the first discovery, several families of iron-pnictide have appeared such as $LnFeAs(O, F)$ or $LnFeAsO_{1-x}$ with T_c up to 56 K, referred to as 1111 pnictide [24], $(Ba, K)Fe_2As_2$ with T_c values range up to 38 K referred to as 122 pnictide [25, 26] and $LiFeAs$ with T_c up to around 20 K, referred to as 111 compounds [27]. because of the new compounds are very different from the cuprate superconductor and may help introduce to a theory of non-BCS theory superconductivity they are very important.

3.1.1 Crystal and Electronic Structure

The crystal structures of the Four families of Iron-pnictides are:

1111 family

LaFeAsO and the 1111 family of Iron-pnictides crystallizes in the ZrCuSiAs type structure, (space group P4/nmm). In this structure, two-dimensional layers of edge- sharing $FeAs_{4/4}$ tetrahedral alternate with sheets of edge-sharing $LaO_{4/4}$ tetrahedral as shown in Fig 3.1 (a) [18]. Because of the differences between the ionic nature of the Ln-O (Lanthanum oxide) bonds and the more covalent Fe-As (iron arsenide) bonds, a distinctive two-dimensional structure forms, where ionic layers of lanthanum oxide $(LaO)^+$ alternate with metallic layers of iron arsenide $(FeAs)^-$.

122 family

The ternary iron arsenide $BaFe_2As_2$, with the tetragonal $ThCr_2Si_2$-type structure space group (space group I4/nmm) contains practically identical layers of edge- sharing $FeAs_{4/4}$ tetrahedra, but they are separated by barium atoms instead of LaO sheets. This structure is shown in Fig 3.1(b) [25].

111 family

LiFeAs crystallizes into a Cu_2Sb-type tetragonal structure containing [FeAs] layer with an average iron valence Fe^{2+} like those for 1111 or 122 parent compounds. This structure is shown in Fig 3.1 (c) [28].

11 family

The PbO-type $\alpha FeSe$ crystal structure is shown in Fig 3.1 (d) [29].

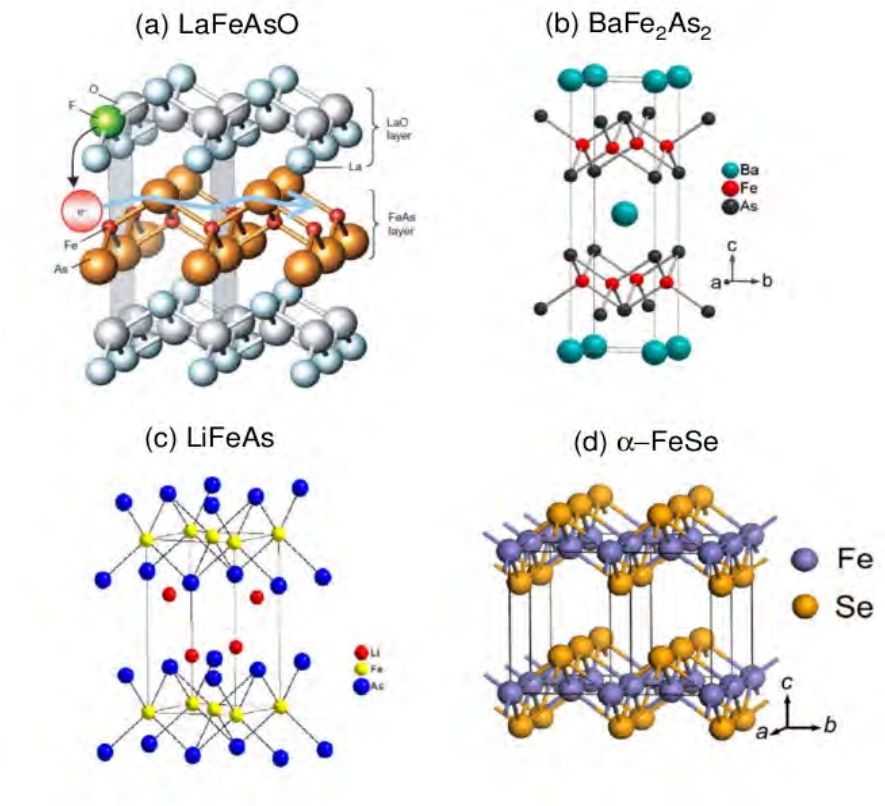

Figure 3.1: Schematic Crystal structure of: (a) LaFeAsO , (b)$BaFe_2As_2$ (c) LiFeAs (d) $\alpha FeSe$.

The First principles electronic structure calculation of the $LaOFeP$ compound, in which superconductivity ($T_c = 4K$) had been first found, was done before the discovery of high T_c values in this class of compounds [30]. Electronic structure analysis show that the Fermi surface and band structures of the different families of iron-pnictides are quite generally identical. In this section, we show selected results from literature in which the electronic structure of the various families of pnictides are calculated.

•LaFeAsO and LaFePO

Electronic structure calculation of the $LaOFeP$ and $LaFeAsO$ compound which is performed by V. Vildosola et al. [31] to study and compare the two compounds was accomplished in the interest of clarifying the connections between electronic properties and the electronic

structure of these materials. the attained band structures for both materials using experimental crystal structure. It is clear that the bands near the Fermi level which correspond to Fe, have larger bandwidth in $LaFePO$ as compared to $LaFeAsO$. Very low-energy band structure and Fermi surfaces studies for both compounds exhibit that in both compounds, the Fermi level is crossed by five bands with mainly **Fe** character.

• **Ba** Fe_2As_2

The calculated (Local Density Approximation) LDA band-structures and Fermi surfaces of $BaFe_2As_2$ by D. J. Singh [32] presents a clear observation of high DOS near E_F with the major supplement comes from Fe 3d states and also three dimensionality in the electronic structure of $BaFe_2As_2$.

It must also be remarked that, aside from the common general characteristics in the electronic structures of iron pnictides, many differences exit in 122 family. For example, the calculations of F. Ma et al [33] indicated many differences in the band structures and Fermi surfaces between various compounds of 122 family such as $BaFe_2As_2$, $SrFe_2As_2$, and $CaFe_2As_2$.

• **LiFeAs**

These calculations are taken from the same reference as above from D.J. Singh [32]. The electronic structure of LiFeAs has the general features of other FeAs materials: Small Fermi Surfaces, with hole cylinders at the BZ center and electron cylinders at the BZ corner, high DOS near E_F and strongly increasing DOS below E_F. However, the hole-like Fermi Surfaces at the BZ center is less three-dimensional than that of $BaFe_2As_2$.

3.1.2 Magnetic structure and phase diagram

$LaOFeAs$ compounds are easy structure, of alternating layers of Fe-As and La-O layers where FeAs layers are believed to be responsible for superconductivity. The main compound or undoped compound of these systems is not superconducting itself and exhibits both a structural and magnetic phase transition. This structural phase transition alters the crystal symmetry from tetragonal (space group P4/nmm) to orthorhombic (space group Cmma) and leads to an antiferromagnetical order with a spin structure, which is shown in Figure (3.2).

However, the first direct existence of SDW order in $LaFeAsO$ came from neutron-scattering experiments by de la Cruz et al. [34]. These experiments exposed that $LaFeAsO$ undergoes a direct structural distortion below ∼155 K changing the symmetry from tetragonal (space group P4/nmm) to monoclinic (space group P112/n) at low temperatures, and then, at ∼137 K, produces long-range SDW-type antiferromagnetic (AFM) order with a small moment but simple magnetic structure. The magnetic structure is undeviating with theoretical predictions, but the moment of 0.36(5)μB per iron atom noticed here at 8 K is much smaller than the predicted value of ∼2.3 μ B per iron atom. Later, the AFM order in $BaFe_2As_2$ was also surveyed by a neutron diffraction study by Huang et al. [35]. Similar to the case of $LaFeAsO$, $BaFe_2As_2$ shows a tetragonal to orthorhombic distortion structural transition and magnetic transition. However, both transitions occur simultaneously in $BaFe_2As_2$ in contrast with the separated transitions observed previously in $LaFeAsO$. These results for both compounds are summarized in Figure. 3.2.

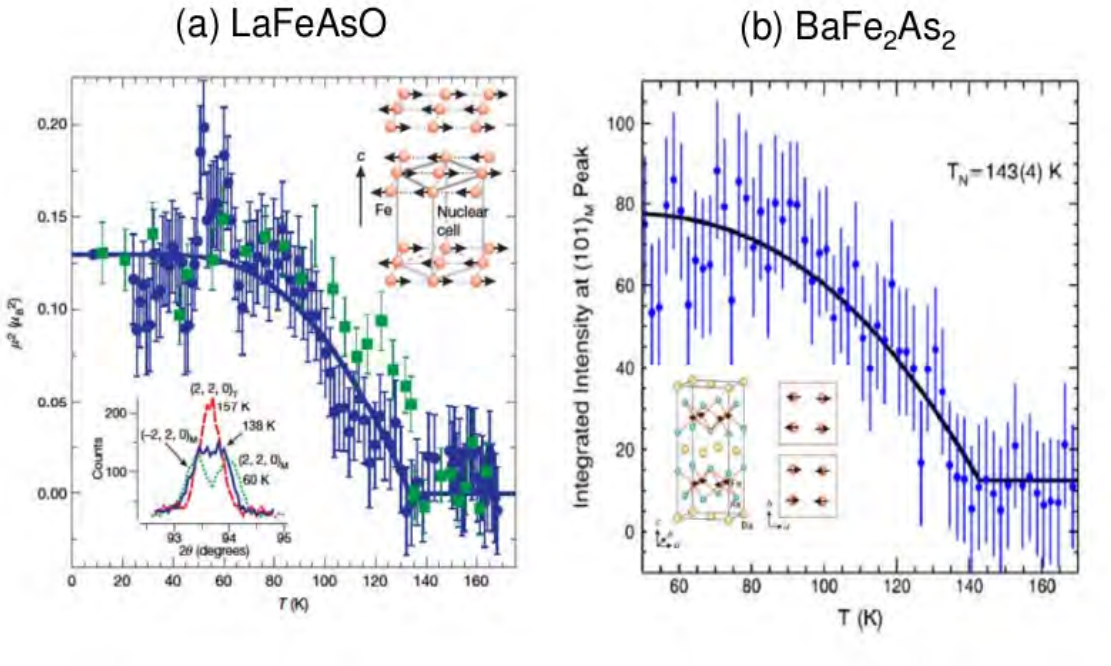

Figure 3.2: Antiferromagnetic ordering in (a)LaFeAsO and (b)$BaFe_2As_2$.

3.1.3 Spin Density Wave(SDW)

Spin-density wave (SDW) are low-energy ordered states of solids, which occur at low temperature in anisotropic, low-dimensional materials or in metals that have high densities of states at the Fermi level $N(E_f)$. Other low-temperature ground states that occur in such materials are superconductivity, ferro-magnetism and antiferro-magnetism.

The spin-density wave(SDW) state is a kind of antiferromagnrtic state with the electronic, spin density establishing a static wave. The density varies rhythmically as a function of the position (r) with no net magnetization in the total volume.

Specifically, spin-density wave(SDW) occurs with spacial spin-density modulation due to delocalized or itinerant electron rather than localized ones. In the normal state the density $\rho_\uparrow(r)$ of electron polarized upward with respect to any quantization axis is completely canceled by the density $\rho_\downarrow(r)$ of downward polarized spin.

In the spin-density wave(SDW), however the difference $\sigma(r)$ between $\rho_{\uparrow}(r)$ and $\rho_{\downarrow}(r)$ is finite and oscillates in space as a function of the position vector (r) in spin-density wave(SDW) state (Organic superconductors, vo1.88).

$$\sigma(r) = \rho_{\uparrow}(r) - \rho_{\downarrow}(r) \tag{3.1}$$

3.1.4 Coexistence of S.D.W and Superconductivity

The FeAs based new superconductors have generated great enthusiasm, since the superconducting transition temperature T_c of these alternating layer materials increases to above 40 K and finally reaches about 55 K. In addition to the superconductivity, a closely related electron pair imbalance on the Fermi surface, the spin-density wave (SDW), has been deduced from the nesting Fermi surface and recognized directly in neutron diffraction experiments in both $LaFeAsO$ (1111) and $BaFe_2As_2$ (122) classes of materials. It is hard to visualize that the same electronic state would take part in both the superconducting and spin-density wave (SDW) electron pairs instability of the Fermi surface, and indeed the electron and hole-like Fermi sheets in $(Ba, K)Fe_2As_2$ have been observed in the angle-resolved photo-emission spectroscopy (ARPES) study to be influenced by either the SDW or superconducting order in the parent or superconducting i.e x = 0.4 compound, respectively. Thus, it would be extremely significant to examine the relationship between the two correlated electronic states in the phase diagram.

The parent compounds of many of the pnictides are antiferromagnetic metals, which referred to here as the spin density wave (SDW) state. On doping, the magnetic order is decreased where

as superconductivity emerges. Establishing the elaborated phase diagram, and whether these two orders occur successively, is essential.

Coexistence of spin-density wave(SDW) and superconductivity in multiple pnictide materials have been reported. For example, in $Ba_{1-x}K_xFe_2As_2$ an extended region of coexistence with 0.2 $\geq$ x <0.4 with a maximum superconducting transition temperature inside this region of $\sim$ 28 K are observed [36].

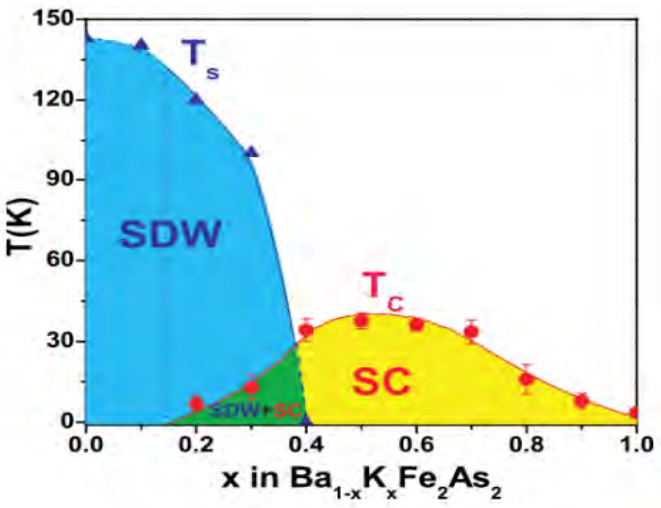

Figure 3.3: The composition-T(k) phase diagram, showing the magnetic and superconducting transitions, T_s denotes the magnetic transition and T_c the superconducting one.

3.1.5 Pairing Symmetry

The knowledge of the pairing symmetry is crucial constituent for explaining the mechanism of superconductivity in iron based superconducting systems.

The pairing symmetry contain significant information on pairing mechanism, Nuclear magnetic resonance measurements have been conducted on 1111 material $LaFeAsO_{0.9}F_{0.1}$ [37] and $PrFeAsO_{0.89}F_{0.11}$ [38], 122 material $BaFe_{1.8}Co_{0.2}As_2$ [39], and 11 structure $FeSe_{0.5}Te_{0.5}$ [40].

All of them showed the Knight shift decreasing below T_c, which indicates spin-singlet Cooper pairing, These confirm the singlet pairing therefore reject odd-parity symmetries such as p-wave state. As a result, $s\pm$-wave and d-wave are more probable according to NMR studies.

Both d-wave and $s\pm$-wave have internal π-phase shifts. The difference is if the π-phase shift is direction-dependent or not. Also they part of different symmetry classes. Scanning SQUID microscopy measurement on $NdFeAsO_{1-x}F_x$ did not observe π-phase shifts between tunneling in different directions, which is contrary to d-wave order [41]. Concurrently, the observation of c-axis Josephson coupling in measurement on $Ba_{1-x}K_xFe_2As_2$ also rules out d-wave pairing symmetry [42] Chen et al. [43] provided a phase-sensitive measurement through the observation of both integer and half-integer flux-quantum transitions in a composite $Nb-NdFeAsO_{0.88}F_{0.12}$ superconducting loop to establish a π-phase shift in the order parameter. This supports a sign change in the gap structure against conventional s-wave. These phase-sensitive experiments show strong evidence of the sign-reversed s-wave symmetry.

Another phase-sensitive measurement using scanning tunneling microscopy on the 11 structure Fe(Se,Te) to image the quasi-particle scattering interference patterns in the superconducting state was reported [44, 45]. By observing the magnetic-field dependence of the quasiparticle scattering strength, Hanaguri et al. [44] found the sign of the gap is reversed between the hole and the electron pockets, favoring $s\pm$-wave.

The magnetic resonance mode is observed in 1111 material [46], more in 122 material [47, 48], and in 111 system [49, 50]. The observation of magnetic resonance mode points to a sign-reversed gap structure.

ARPES reported the observation of three dimensional gap [51]. Therefore, the gap struc-

ture in iron-based superconductors is complex and diverse. Large amount of experiments are consistent with $s\pm$-wave symmetry, which can be fully gaped or nodal $s\pm$-wave. Therefore the observation of in-plane nodes does not clash with this symmetry type. At the end of the discussion we need to consider that the gap symmetry is not conclusive yet.

3.1.6 Mechanism of Superconductivity

Electron-phonon coupling is not sufficient to explain superconductivity in the whole family of iron-based superconductors based on the experiment done for the F-doped LaFeAsO compounds, even smaller coupling constants are predicted [52].

As mentioned above, theoretical calculations indicate that the electron–phonon interaction is not strong enough to give rise to high T_c from a general standpoint, the interplay of magnetism and superconductivity strongly suggests that magnetic fluctuations are involved either directly or indirectly in the Cooper pairing in the Iron Based Superconductors. In the context of magnetism, pairing could arise from fluctuations emanating from a quantum critical point or a more complicated scenario involving the optimal combination of three players - Coulomb repulsion, spin fluctuations and phonon coupling - may favor high-T_c superconductivity in these materials.

phonon's alone were quickly ruled out as a standalone contender for the pairing mediator. A calculation of electron-phonon coupling from first principles helped to conclude that LaFeAsOF is intrinsically at most a very poor electron-phonon superconductor [52]. However, a recalculation of this quantity results in a potential increase of the coupling constant by up to 50% when the effects of magnetism are included [53]. The classic isotope effect experiment,

which provided the first strong evidence for phonon-mediated Cooper pairing in conventional superconductors, is a well-known method of probing the role of phonon's, found an absence of any O isotope effect in $SmFeAsO_{1-x}F_x$, but did find a significant Fe isotope effect ("α" exponent of $\sim$0.35) on both the magnetic and superconducting transitions in both $SmFeAsO_{1-x}F_x$ and $Ba_{1-x}K_xFe_2As_2$ [54] suggesting that phonon's are at least intermediate players. however many people suggests combined phonon-exciton mechanism could explain the T_c values very well as it is believed that the coupling is strong in iron based superconductors, P. Singh et al also proposed that bi-exciton may be involved in pairing mechanism [55].

Many theoretical approaches found that strong antiferromagnetic correlation (spin fluctuation) triggers $s\pm$ pairing next to the antiferromagnetism. The match between spin fluctuation structure and fermiology might drive superconductivity in at least some of these materials. Therefore, antiferromagnetic spin fluctuations could possibly be the major mediating glue in the iron-based superconductors [56, 57, 58, 59].

3.1.7 Factors Affecting Tc in Ferropnictides

Electron Doping and Hole Doping

Substituting of oxygen atom by fluorine or by oxide vacancies, an extra electron goes into the FeAs layer, such situation is commonly referred to as electron doping. A re-distribution of electrons between the doped LaO and FeAs layers gives rise to a conductivity of a compound. Another remarkable fact was a discovery of high-T_c superconductivity in the compounds LaOFeAs without fluorine doping, but under oxygen deficiency. Thus, H. Mukuda et al [60] reports a detection of high T_c values in $LaO_{0.6}FeAs$ (T_c = 28 K), $LaO_{0.75}FeAs$(T_c = 20 K), and $NdO_{0.6}FeAs$ (T_c = 53 K).

The table below represents the different rare earth materials shows different transition temperature with fluorine doping and with oxygen deficiency. The Original compound is $LaF_xO_{1-x}FeAs$ with T_c = 26K.

Flourine doped

$CeO_{1-x}F_xFeAs$	41K
$PrO_{1-x}F_xFeAs$	52K
$NdO_{1-x}F_xFeAs$	51K
$SmO_{1-x}F_xFeAs$	43K
$GdO_{1-x}F_xFeAs$	36K

Doping by oxygen deficency

$LaO_{1-x}FeAs$	31K
$SmO_{1-x}FeAs$	55K
$CeO_{1-x}FeAs$	46K
$NdO_{1-x}FeAs$	53K
$PrO_{1-x}FeAs$	51K

Table 3.1: Transition temperature of fluorine doped and oxygen deficient of different rare earth materials.

Substitution of La^{3+} in LaOFeAs by Sr^{2+}, in such situation we deal with hole doping. The resulting compound, $La_{1-x}Sr_xOFeAs$, at x = 0.13 becomes superconducting with T_c =

25 K [61]. This was the first superconductor in the FeAs based superconductors, obtained by hope doping, as has been confirmed by measuring the Hall coefficient [62]. A system $Pr_{1-x}Sr_xOFeAs$ is another example of the hole doping, on substituting Pr^{3+} by Sr^{2+} [63]. A superconductivity of $T_c = 16.3$ K was achieved at the Sr concentration $x \approx 0.20 - 0.25$.

Electron and Hole Doping is also possible for Ternary Iron Arsenide ($A^{2+}Fe_2As_2$), such as by doping $BaFe_2As_2$ with potassium. The charge carriers in $Ba_{1-x}K_xFe_2As_2$ are holes, which is confirmed by Hall effect measurements. Due to closeness of atomic radii of Ba and K, a complete substitution of the one by the other is possible, so that the $(Ba_{1-x}K_x)Fe_2As_2$ compound can be obtained in the whole range $0 < x < 1$. The measurements have shown that superconductivity exists throughout broad x range but the maximum value $T_c = 38$ K occurs for x = 0.4. A discovery of superconductivity in $BaFe_2As_2$ under electron doping, induced by a substitution of Fe atoms by Co forming $Ba(Fe_{1-x}Co_x)_2As_2$ has been constructed At low Co concentration. The superconductivity appears at $x \approx 0.025$ and persists till concentrations $x \approx 0.16$.

To conclude above discussion the superconductivity in Quaternary Rare earth Iron Arsenide systems might be induced either by electron doping (substituting oxygen by fluorine or due to the presence of oxygen vacancies), or by hole doping via substituting La by Sr. These tendencies are maintained throughout the whole class of the ReOFeAs systems, also the superconductivity in Ternary Iron Arsenide systems might be induced either by electron doping (substitution of Fe atoms by Co), or hole doping (substitution of Ba atoms by K).

Rare-earth elements

In REOFeAs compounds the superconductivity was identified in $LaO_{1-x}F_xFeAs$ with 26 K with F-doping. After that many group substituted La with other rare earths like, Sm, Nd, Ce, Gd, Pr, Tb and Dy according to the simple chemical formula $RE^{+3}O^{-2}Fe^{+2}As^{-3}$. Exchanging lanthanum with rare earth ions of smaller atomic radii in $LnOFeAs$, T_c was found to increased. According to report from experiment the lattice constants, hence the volume, decrease monotonically as the atomic number increases, but T_c increases only from La to Gd, whereupon drops for heavier rare earths. Electronic calculations for Ce, Nd and Gd shows similar DOS and band structure with LaOFeAs however, The effect of size (hence a, c, and the internal coordinates) influences not only the band structure and DOS, but also the magnetic properties.

element	Z	a(Å)	c(Å)	V(Å^3)	T$_{C,onset}$ (K)
La	57	4.033	8.739	142.14	31.2
Ce	58	3.998	8.652	138.29	46.5
Pr	59	3.985	8.595	136.49	51.3
Nd	60	3.965	8.572	134.76	53.5
Sm	62	3.933	8.495	131.40	55.0
Gd	64	3.915	8.447	129.47	56.3
Tb	65	3.899	8.403	127.74	52
Dy	66	3.843	8.284	122.30	45.3

Table 3.2: The different rare earth ion superconductors with Transition temperature.

Pressure

It was found that pressure has a large effect on iron pnictides so that some parent compounds can become superconducting by simply applying pressure. As an example of the pressure effect,

we remark that the T_c of the original system $LaO_{1-x}F_xFeAs$ went up from 26 K to ∼43 K by applying a pressure of ∼4 GPa [18]. It was suggested that the lattice compression is responsible for this effect. Indeed, in ReOFeAs compounds the atoms of rare-earth element have smaller radius than La, and T_c in these compounds is markedly higher, exceeding 50 K. In a subsequent work, the measurements of electrical conductivity in LaOFeAs under high pressures, up to 29 GPa, have been done [64].

As is seen from Fig. 3.4, the maximal T_c = 21 K in stoichiometric compound LaOFeAs is achieved at the pressure of 12 GPa. As regards the variation of T_c with pressure in doped compounds, it first rises with pressure, passes through maximum and falls down. A similar behaviour of T_c under pressure is observed in $LaO_{1-x}F_xFeAs$ of a different composition, a similare trand shown in oxygen deficient LaOFeAs compounds [18].

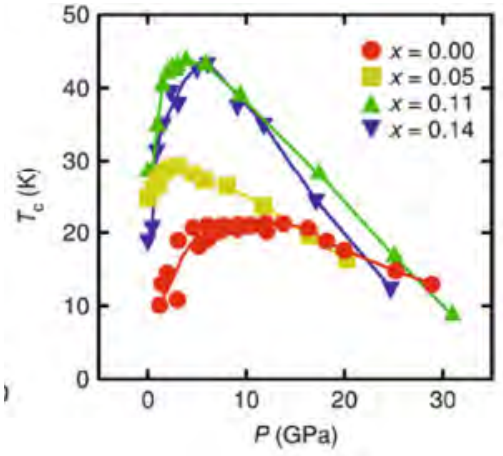

Figure 3.4: Variation of T_c with pressure in $LaO_{1-x}F_xFeAs$ compounds.

A relation between the changes of T_c under pressure and variation of the lattice parameter at high pressures ($P > 10GPa$), the lattice parameters and T_c for the compound investigated $LaO_{0.9}F_{0.1}FeAs$ do decrease linearly [65].

In AFe_2As_2 compounds the application of pressure suppresses both the structural and

the magnetic transitions and leads to the superconductivity. The high pressure experiment indicates that superconductivity appears at approximately 2 GPa to 6 GPa for $BaFe_2As_2$ and has a peak of T_c = 29 K near 4GPa [66], $SrFe_2As_2$ was first reported to superconducts at 2.5 GPa pressure with T_c =27 K [66] and T_c decreases to below 20K with further increasing pressure up to 5.2 GPa.

The main effect of pressure on the crystal structure of AFe_2As_2 is to shorten the Fe-Fe and Fe-As bond length and As-Fe-As bond angles. The angle changes slightly with a slight change in $FeAs_4$ tetrahedra, which is not equal to that of doped structure. In doped $A_{1-x}K_xFe_2As_2$ the tetrahedral angle is about 109.5° which is ideal tetrahedral angle for superconductitivity, and transition temperature can reach value up to T_c = 38K. While the parent compound under pressure the significant transition temperature can reach value up to 28K.

Chapter 4

Current Status of Iron-based Superconductors

4.1 Recent Studies on Iron based superconductor

In this Chapter, we see the progress of study of Iron based superconductors.

As mentioned earlier the superconductivity of the 1111-type materials was first discovered in $LaFePO$ by Kamihara et al. in 2006, with a relatively low T_c of 4 K; this T_c could be enhanced to 7 K by fluorine doping at the oxygen sites, which produces more electron carriers in the crystal lattice. This report was not widely noted until a breakthrough appeared in February 2008, when the same research group announced a similar superconductor of F-doped $LaFeAsO_{1-x}F_x$, with T_c reaching 26 K when x is around 0.11. The undoped parent compound, $LaFeAsO$, was investigated but showed no superconductivity at low temperature. This relatively high T_c of 26 K, the iron-containing composition, and the layered crystal structure became immediate topics of interest and research. By replacing the La atoms with other rare-earth elements and

modulating the structural parameters, new superconductors were discovered and T_c was quickly enhanced in $SmFeAsO_{1-x}F_x$, $CeFeAsO_{1-x}F_x$, $PrFeAsO_{1-x}F_x$, and $NdFeAsO_{1-x}F_x$ to above 50 K. The succeeding investigation has seen a doubling of the highest onset T_c (from resistance measurements) of the 1111-type superconductors up to 55–57 K as reported by several groups.

Apart from the 1111-type, other structural types of iron-based superconductors were also synthesized, all of them with a T_c lower than 40 K. These iron-based pnictide superconductors have been named the second class of the high-T_c family after cuprate superconductors. One structural case is the ternary $ThCr_2Si_2$-type compounds (denoted as 122-type), which belong to a very old family with much richer chemical composition. Superconductivity in these 122-type compounds has been found in $LaIr_2Ge_2$, $LaRu_2P_2$ and $BaNi_2P_2$ with T_c being low, at about several degrees Kelvin. Among the FeAs-based 122-type superconductors, K-doped $(Ba_{1-x}K_x)Fe_2As_2$, which has a remarkable T_c of 38 K when x = 0.4 . was the first to be discovered. Other 122-type compounds, such as doped $CaFe_2As_2$, $SrFe_2As_2$, and $EuFe_2As_2$, were also found to be superconducting but with lower T_c.

Other reported compounds that superconducts at low temperature include $FeSe_{1-x}$, Li_xFeAs, $La_3Ni_4P_4O_2$, denoted 11-type, 111-type, and 3442-type, respectively. The simplest compound is the PbO-type $FeSe_{1-x}$, which was formed by Fe-Se layers repeatedly stacked together; its T_c is 8 K. The 111-type Li_xFeAs and Na_xFeAs compounds, with T_c can reach 18 K. A special Ni–P-based compound, $La_3Ni_4P_4O_2$, was also reported to have a T_c of 2 K.

A summary of more than 70 iron-based superconductors is reported and I provided it in Table. Here we note that the named Fe-based superconductors include all the Fe-As, Fe-P, Fe-Se, Ni-As, Ni-P based and related superconductors in this review.

Experimental facts indicate that the FeAs-based superconductors have a much higher T_c than others and furthermore, only the 1111-type Fe–As-based superconductors exhibited a high T_c above 40 K. At present it is not clear whether all types of iron-based superconductors share the same superconducting mechanism or not.

Although theoretical calculations have indicated similar electronic band structures, some Ni–As-based superconductors have been shown to exhibit conventional superconducting behavior. but almost all of the shows unconventional superconducting mechanism.

Compound	T_c [K]	Compound	T_c [K]
$LaFePO$	5	$La_{1-x}Sr_xFeAsO$	25
$LaNiPO$	3	$Pr_{1-x}Sr_xFeAsO$	16.3
$PrFePO$	3.2	$Nd_{1-x}Sr_xFeAsO$	13.5
$NdFePO$	3.1	$La_{1-x}Sr_xNiAsO$	3.7
$SmFePO$	3	$LaNiAsO$	2.4
$LaFeAsO_{1-x}F_x$	26, 41	$LaNiAsO_{1-x}F_x$	3.78
$SmFeAsO_{1-x}F_x$	43, 55	$LaFeAsO_{1-x}P_x$	10.5
$CeFeAsO_{1-x}F_x$	41	$LaFeAsO$	21 (HP)
$PrFeAsO_{1-x}F_x$	52	$LaIr_2Ge_2$	1.5
$NdFeAsO_{1-x}F_x$	52	$LaRu_2P_2$	4.1
$GdFeAsO_{1-x}F_x$	52	$YIr_{2-x}Si_{2-x}$	2.5
$TbFeAsO_{1-x}F_x$	46	$BaNi_2P_2$	3
$DyFeAsO_{1-x}F_x$	45	$Ba_{1-x}K_xFe_2As_2$	38

Compound	T_c [K]	Compound	T_c [K]
$YFeAsO_{1-x}F_x$	10	$BaFe_{2-x}Ni_xAs_2$	20.5
$EuFeAsO_{1-x}F_x$	11	$Sr_{1-x}Cs_xFe_2As_2$	37
$LaFeAsO_{1-x}$	31, 43	$Sr_{1-x}K_xFe_2As_2$	37
$CeFeAsO_{1-x}$	46.5	$Ca_{1-x}Na_xFe_2As_2$	20
$PrFeAsO_{1-x}$	51.3	$EuFe_2As_{2-x}P_x$	26
$NdFeAsO_{1-x}$	53.5	$Eu_{0.5}K_{0.5}Fe_2As_2$	32
$SmFeAsO_{1-x}$	55	$Eu_{1-x}Na_xFe_2As_2$	34.7
$GdFeAsO_{1-x}$	53.5	$BaFe_{2-x}Co_xAs_2$	22
$TbFeAsO_{1-x}$	48.5	$CaFe_{2-x}Co_xAs_2$	17
$DyFeAsO_{1-x}$	52.2	$SrNi_2As_2$	0.62
$HoFeAsO_{1-x}$	50.3	$BaNi_2As_2$	0.7
$YFeAsO_{1-x}$	46.5	$CsFe_2As_2$	2.6
$Gd_{1-x}Th_xFeAsO$	56	$BaFe_2As_2$	29 (HP)
$Tb_{1-x}Th_xFeAsO$	52	$SrFe_2As_2$	27 (HP)
$SmFe_{1-x}Co_xAsO$	17.2	$CaFe_2As_2$	12 (HP)
$LaFe_{1-x}Co_xAsO$	14.3	KFe_2As_2	3.8
$CeFe_{1-x}Co_xAsO$	11.3	$BaIr_2P_2$	2.1
$CaFe_{1-x}Co_xAsF$	22	$BaRh_2P_2$	1.0
$SrFe_{1-x}Co_xAsF$	4	$SrNi_2P_2$	1.4
$Sr_{1-x}La_xFeAsF$	29.5	$LiFeAs$	18
$Sr_{1-x}Sm_xFeAsF$	56	$NaFeAs$	9

Compound	T_c [K]	Compound	T_c [K]
$Ca_{0.4}Nd_{0.6}FeAsF$	57.4	$FeSe$	8,37 (HP)
$La_{1-x}Pb_xOFeAs$	11.6	$FeSe_{1-x}Te_x$	14
$Ca_{0.4}Pr_{0.6}FeAsF$	52.8	$FeTe_{1-x}S_x$	10
$Sm_{0.95}La_{0.05}O_{0.85}F_{0.15}FeAs$	57.3	$FeSe_{1-x}S_x$	15.5
$LaNiBiO$	4	$La_3Ni_4P_4O_2$	2.2

Chapter 5

Application of Superconductors

5.1 Application of Iron-based Superconductors

The recent discovery of iron-based superconductors has provoked eagerness for extensive research on these materials because they form the second high-temperature superconductor family after the copper oxide superconductors and impart an expectation for materials with a higher transition temperature. It has also been clarified that they have exceptionally unusual physical properties such as unconventional pairing mechanism and superconducting properties preferable for application with high upper critical field and small anisotropy.

Iron-based Superconducting Wire

The development of an iron-based superconductor that Hosono's research group reported three years ago is a remarkable achievement, producing a superconductor with a maximum transition temperature of 56 K, although it is below the highest recorded transition temperature of a copper oxide-based superconductor, iron-based superconductors have a large upper critical field of 50-100 T, along with a small anisotropy compared to copper oxide-based su-

perconductors, it is highly anticipated that wire applications involving magnets that generate large magnetic fields exceeding those of metal-based superconducting wires will emerge.

Currently, the T_c of an iron-based superconductor is lower compared to a copper oxide-based superconductor. Thus, a Y-based copper oxide thin film operating at a T_c greater than 90 K exhibits greater critical current density values when compared at the same temperature. However, the characteristics of Iron-based superconductors, including their smaller anisotropy, high tolerance for magnetic field, large critical angle are now apparent, with these results implying the great potential for superconducting wires/tapes applications, in particular, wires that are able to generate greater magnetic fields than their metal-based counterparts at low temperatures.

Iron based superconductor Josephson devices

Scientists and engineer's now developing a SIS (superconductor-insulator-superconductor) tunneling Josephson junctions using newly discovered iron-based superconductors that is the basic component of superconducting devices. With the development of high-T_c SQUID (superconducting quantum interference device) magnetometers that operates at temperatures higher than conventional, this research aims at applications involving ultra-sensitive biomagnetic measurement such as magnetocephalography and magnetocardiography.

Iron-based high-temperature superconducting devices are expected to operate at high temperatures, speeds and frequencies incomparable with conventional devices. With conventional copper oxide high-temperature superconducting, devices are considered to be infeasible unless the interfaces are controlled, but a technology for creating junctions has not been established. iron-based high-temperature superconductors have excellent lattice matching with Si and III-

V-group semiconductors. They are also compatible with semiconductor processing technology. Therefore, in addition to the short term target of developing a SQUID.

This technology is very promising for manufacturing integrated devices, in the future Iron-based superconductor device will provide the basis for "post-niobium" superconductivity electronics to replace the niobium-based devices today.

Bibliography

[1] H.K. Onnes,*"On the sudden change in the rate at which the resistance of mercury disappears,".Comm. Leiden.* November 25, (1911).

[2] W. Meissner and R. Ochsenfeld, *Naturwiss.* **21**, 787 (1933).

[3] F. London and H. London, *"The electromagnetic equations of the supreconductor," Proc. Roy. Soc.* (London) **A149**, 71 (1935).

[4] V.L. Ginzburg and L.D. Landau,*"On the theory of superconductivity," Zh. Eksp. Teor. Fiz.* **20**, 1064 (1950).

[5] H. Fröhlich,*Phys. Rev.* **79**, 845–856 (1950).

[6] E. Maxwell,*"Isotope effect in the superconductivity of mercury," Phys. Rev.* **78**, 477 (1950).

[7] J. Bardeen and D. Pines,*Phys. Rev.* **99**, 1140–1150 (1955).

[8] J. Bardeen, L.N. Cooper and J.R. Schrieffer, *"Theory of superconductivity," Phys. Rev.* **108**, 1175 (1957).

[9] J.G. Bednorz, K.A. Mueller, *"Possible high TC superconductivity in the Ba-La-Cu-O system," Zeitschrift für Physik B.* **64** (2): 189–193(1986).

[10] R.J. Cava, A. Santoro, D.W. Johnson, Jr., and W.W. Rhodes,*"Crystal structure of the high- temperature superconductor La1.85Sr0.15CuO4 above and below Tc," Phys. Rev. B* **35**, 6716 (1987).

[11] C.W. Chu, J. Bechtold, L. Gao, P.H. Hor, Z.J. Huang, R.L. Meng, Y.Y. Sun, Y.Q. Wang, and Y.Y. Xue,*"Superconductivity at 90 K in a Y-Ba-Cu-O Compound System," Phys. Rev. Lett.* **60**, 941 (1988).

[12] H. Maeda, Y. Tanaka, M. Fukutumi, and T. Asano, *"A New High-Tc Oxide Superconductor without a Rare Earth Element," Jpn. J. Appl. Phys.* **27** (2): L209–L210 (1988).

[13] Z.Z. Sheng, A.M. Hermann,*"Bulk superconductivity at 120 K in the Tl–Ca/Ba–Cu–O system," Nature.* **332** (6160): 138–139 (1988).

[14] C.W. Chu et al, *"Superconductivity above 150 K in $HgBa_2Ca_2Cu_3O_8$ at high pressures," Nature.* **365** (6444): 323 (1993).

[15] L. Gao et al, *"Superconductivity up to 164K in $HgBa_2Ca_{m-1}Cu_mO_{2m+2}$ under quasihydrostatic pressures," Phys.Rev B.* **50** (6) 4260–4263 (1994).

[16] Y. Kamihara, H. Hiramatsu, M. Hirano, R. Kawamura, H. Yanagi, T. Kamiya, and H. Hosono, *"Iron-Based Layered Superconductor: LaOFeP," J. Am. Chem. Soc.* **128** (31): 10012–10013 (2006).

[17] Y. Kamihara, T. Watanabe, M. Hirano, and H. Hosono,*"Iron-Based Layered Superconductor La[O1-xFx] FeAs (x = 0.05−0.12) with Tc = 26 K," J. Am. Chem. Soc.* **130** (11) (2008).

[18] H. Takahashi, K. Igawa, K. Arii, Y. Kamihara, M. Hirano, and H. Hosono, *"Superconductivity at 43 K in an iron-based layered compound $LaO_{1-x}F_xFeAs$," Nature.* **453** 376 (2008).

[19] G.F. Chen, Z. Li, D. Wu, G. Li, W.Z. Hu, J. Dong, P. Zheng, J.L. Luo, and N.L. Wang, *"Superconductivity at 41 K and Its Competition with Spin-Density-Wave Instability in Layered CeO1- xFxFeAs," Phys. Rev. Lett.* **100**, 247002 (2008).

[20] Z.A. Ren, J. Yang, W. Lu, W. Yi, G.C. Che, X.L. Dong, L.L. Sun, Z.X. Zhao, *"Superconductivity at 52 K in iron based F doped layered quaternary compound Pr[O1–xFx]FeAs ," Materials Research Innovations.* **12**, (3), 105-106(2) (2008).

[21] Ren Zhi-An, Lu Wei, Yang Jie, Yi Wei, Shen Xiao-Li, Li Zheng-Cai, Che Guang-Can, Dong Xiao-Li, Sun Li-Ling, Zhou Fang, Zhao Zhong-Xian, *"Superconductivity at 55 K in iron-based F-doped layered quaternary compound Sm[O1-xFx]FeAs," Chin. Phys. Lett.* **25**, 2215 (2008).

[22] B.S. Deaver and W.M. Fairbank, Bascom, Fairbank, William, *"Experimental Evidence for Quantized Flux in Superconducting Cylinders," Phys. Rev. Lett.* **7** (2): 43 (1961).

[23] R. Doll and M. Nabauer, R. Näbauer, *"Experimental Proof of Magnetic Flux Quantization in a Superconducting Ring," Phys. Rev. Lett.* **7** (2): 51 (1961).

[24] Z.H. Ren et al, *"Superconductivity and phase diagram in iron-based arsenic-oxides $ReFeAsO_{1-x}$ without fluorine doping," Chin. Phys. Lett.* **83** 17002 (2008).

[25] M. Rotter, M. Tegel, and D. Johrendt, *"Superconductivity at 38 K in the Iron Arsenide $(Ba_{1-x}K_x)Fe_2As_2$," Phys. Rev. Lett.* **101** (10): 107006 (2008).

[26] K. Sasmal et al, *"Superconducting Fe-Based Compounds $(A_{1-x}Sr_x)Fe_2As_2$ with K and Cs with Transition Temperatures up to 37 K," Phys. Rev. Lett.* **101** (10) (2008).

[27] J.H. Tapp et al, *"LiFeAs An intrinsic FeAs-based superconductor with Tc=18 K," Phys. Rev. B.* **78** (6): 060505 (2008).

[28] X.C. Wang, Q.Q. Liu, Y.X. Lv, W.B. Gao, L.X. Yang, R.C. Yu, F.Y. Li, C.Q. Jin, *"The superconductivity at 18 K in LiFeAs system,"* Sol. Sta. Comm. **148** 538 (2008).

[29] F.C. Hsu, J.Y. Luo, K.W. Yeh, T.K. Chen, T.W. Huang, P.M. Wu, Y.C. Lee, Y.L. Huang, Y.Y. Chu, D.C. Yan and M.K. Wu, *"Superconductivity in the PbO-type structure α-FeSe,"* Proc. Natl. Acad. Sci. **105** 14262 (2008).

[30] S. Lebeque, *"Electronic structure and properties of the Fermi surface of the superconductor LaOFeP,"* Phys. Rev. B. **75** 035110 (2007).

[31] V. Vildosola, L. Pourovskii, R. Arita, S. Biermann and A. Georges, *"Bandwidth and Fermi surface of iron oxypnictides: Covalency and sensitivity to structural changes,"* Phys. Rev. B. **78** 064518 (2008).

[32] D.J. Singh, *"Electronic structure and doping in $BaFe_2As_2$ and LiFeAs: Density functional calculations,"* Phys. Rev. B. **78** 094511 (2008).

[33] F. Ma, Z. Lu, and T. Xiang, *"Electronic structures of ternary iron arsenides AFe_2As_2 (A=Ba,Ca or Sr),"* arXiv: 0806.3526.

[34] C. de la Cruz, Q. Huang, J.W. Lynn, J. Li, W. Ratcliff II, J.L. Zarestky, H.A. Mook, G.F. Chen, J.L. Luo, N.L. Wang and P. Dai, *"Magnetic order close to superconductivity in the iron-based layered $LaO_{1-x}F_xFeAs$ systems"* Nature. **453** 899 (2008).

[35] Q. Huang, Y. Qiu, W. Bao, M.A. Green, J.W. Lynn, Y.C. Gasparovic, T. Wu and X. H. Chen, *"Neutron- Diffraction Measurements of Magnetic Order and a Structural Transition in the Parent $BaFe_2As_2$ Compound of FeAs-Based High-Temperature Superconductors,"* Phys. Rev. Lett. **101** 257003 (2008).

[36] H. Chen, Y. Ren et al, *"Coexistence of the spin-density-wave and superconductivity in the $(Ba,K)Fe_2As_2$,"* Europhys. Lett. **85**, 17006 (2009).

[37] H.J. Grafe, D. Paar et al, *"75As NMR studies of superconducting $LaFeAsO_{0.9}F_{0.1}$,"* Phys. Rev. Lett. **101**, 047003 (2008).

[38] K. Matano, Z.A. Ren et al, *"Spin-singlet superconductivity with multiple gaps in $PrFeAsO_{0.89}F_{0.11}$,"* Europhys. Lett. **83** 57001 (2008).

[39] F. Ning, K. Ahilan et al, *"59Co and 75As NMR investigation of electron-doped high T_c superconductor $BaFe_{1.8}Co_{0.2}As_2$,"* J. Phys. Soc. **77** 103705 (2008).

[40] Y. Shimizu, T. Yamada et al, *"Pressure induced antiferromagnetic fluctuations in the pnictide superconductor $FeSe_{0.5}Te_{0.5}$: 125Te NMR study,"* J. Phys. Soc. **78** 123709 (2009).

[41] C.W. Hicks, T.M. Lippman et al, *"Limits on the superonducting order parameter in $NdFeAsO_{1-x}F_y$ from scanning squid miscroscopy,"* J. Phys. Soc. **78** 013708 (2009).

[42] X. Zhang, Y.S. Oh et al, *"Observation of the josephson effect in $Pb/Ba_{1-x}K_xFe_2As_2$ single crystal junctions,"* Phys. Rev. Lett. **102** 147002 (2009).

[43] C.T. Chen, C.C. Tsuei et al, *"Integer and half-integer flux-quantum transitions in a niobium-iron pnictide loop,"* Nat. Phys. **6** 260 (2010).

[44] T. Hanaguri, S. Niitaka et al, *"Unconventional s-wave superconductivity in Fe(Se,Te),"* Science. **328** 474 (2010).

[45] J.E. Hoffman et al, *"Sign flips and spin fluctuations in iron high-T_c superconductors,"* Science. **328** 441 (2010).

[46] S. Shamoto, M. Ishikado et al, *"Inelastic neutron scattering study on the resonance mode in an optimally doped superconductor $LaFeAsO_{0.92}F_{0.08}$,"* Phys. Rev. B. **82** 172508 (2010).

[47] A.D. Christianson, D. Parshall et al, *"Unconventional superconductivity in $Ba_{0.6}K_{0.4}Fe_2As_2$ from inelastic neutron scattering,"* Nature. **456** 930 (2008).

[48] S. Chi, A. Schneidewind et al, *"Inelastic neutron-scattering measurements of a three-dimensional spin resonance in the FeAs-based $BaFe_{1.9}Ni_{0.1}As_2$ superconductor,"* Phys. Rev.Lett. **102** 107006 (2009).

[49] Y. Qiu, W. Bao et al, *"Spin gap and resonance at the nesting wave vector in superconducting $FeSe_{0.4}Te_{0.6}$,"* Phys. Rev. Lett. **103** 067008 (2009).

[50] J. Wen, G. Xu et al, *"Effect of magnetic field on the spin resonance in $FeTe_{0.5}Se_{0.5}$ as seen via inelastic neutron scattering $FeSe_{0.4}Te_{0.6}$,"* Phys. Rev. B. **81** 100513 (2010).

[51] Y.M. Xu, Y.B. Huang et al, *"Observation of a ubiquitous three-dimensional superconducting gap function in optimally doped $Ba_{0.6}K_{0.4}Fe_2As_2$,"* Nat. Phys.**7** 198 (2011).

[52] L. Boeri, O.V. Dolgov, and A.A. Golubov, *"Is $LaFeAsO_{1-x}F_x$ an electron-phonon superconductor?,"* Phys. Rev. Lett. **101** 026403 (2008).

[53] L. Boeri, M. Calandra, I.I. Mazin et al, *"Effects of magnetism and doping on the electron-phonon coupling in $BaFe_2As_2$,"* Phys. Rev. B. **82** 020506 (2010).

[54] R.H Liu, T. Wu et al, *"A large iron isotope effect in $SmFeAsO_{1-x}F_x$ and $Ba_{1-x}K_xFe_2As_2$,"*. Nature. **459** 64 (2009)

[55] P. Singh and K.P. Sinha, *"A possible mechanism of high T_c superconductivity involving biexcitons,"* *J. Sol. Sta. Comm.* **73** 45 (1990)

[56] K. Kuroki, S. Onari et al, *"Unconventional pairing originating from the disconnected fermi surfaces of superconducting $LaFeAsO_{1-x}F_x$,"* Phys. Rev. Lett. **101** 087004 (2008).

[57] A.V. Chubukov, D.V. Efremov et al, *"Magnetism, superconductivity and pairing symmetry in iron-based superconductors,"* Phys. Rev. B. **78** 134512 (2008).

[58] Z.J. Yao, J.X. Li et al, *"Spin fluctuations, interband coupling and unconventional pairing in iron- based superconductors,"* New J. Phys. **11** 025009 (2009).

[59] F.Yang, H.Zhai et al, *"The electronic instabilities of the iron-based superconductors: A variational monte-carlo study,"* Phys. Rev. B. **83** 134502 (2011).

[60] H. Mukuda et al, "75As-NQR/NMR Studies on Oxygen-Deficient Iron-Based Oxypnictide Superconductors LaF eAsO1−y (y = 0, 0.25, 0.4) and N dF eAsO0.6 " J. Phys. Soc. 77 093704 (2008).

[61] Hai Hu Wen et al, "Superconductivity at 25 K in hole-doped (La1−x Srx)OF eAs" Europhys. Lett. 82 17009 (2008).

[62] G. Mu, L. Fang, H. Yang, X. Zhu, P. Che, arXiv: 0806.2104 (2008).

[63] G. Mu, B. Zeng, X. Zhu, F. Han, P. Cheng, B. Shen, H.H. Wen, Phys. Rev. B. 78 104501 (2008).

[64] H. Okada, K. Igawa, H. Takahashi, Y. Kamihara, M. Hirano, H. Hosono, K. Matsubashi,Y. Uwatoko, J. Phys. Soc. Jpn. 77 113712 (2008).

[65] G. Garbarino, P. Toulemonde, M. Alvarez-Murga, A. Sow, M. Mezouar, M. NunezRegueiro, Phys. Rev. B. 78 100507 (2008).

[66] P.L. Alireza, Y.T. Chris Ko, Jack Gillett, C.M. Petrone, and G.G. Lonzarich, "Superconductivity up to 29 K in SrF e2 As2 and BaF e2 As2 at high pressures" arXiv: 0807.1896 (2008).

Declaration

This project is my original work, has not been presented for a degree in any other University and that all the sources of material used for the project have been dully acknowledged.

Name: Nahom Tefera

Signature: _____

University advisor.

Name: Prof P. Singh

Signature: _____

Place and time of submission: **Department of Physics**
Addis Ababa University
June, 2012